Biotribology 19 (2019) 100104

Contents lists available at ScienceDirect

Biotribology

journal homepage: www.elsevier.com/locate/biotri

Tribofilms on CoCrMo alloys: Understanding the role of the lubricant

Mohamad Taufiqurrakhman*, Michael G. Bryant, Anne Neville

Institute of Functional Surfaces (iFS), School of Mechanical Engineering, University of Leeds, LS2 9JT, UK

A B S T R A C T

The tribological activation of a passive metal alloy in an aqueous biological environment have been highlighted by many researchers; better known as bio-tribo-corrosion. Tribocorrosion processes, which can be found at a number of metal-based biomedical implant interfaces, can be affected by lubricant species such as proteins, amino acids and salts. To date, researchers have quantified how the presence of organic species and the environment affect the tribological and corrosion process. However, the nature of the bio-films is still broadly to be explored. This study aims to understand how the lubricant - surface interactions influence the evolving frictional, corrosion and material volume loss from CoCrMo alloys and how the formation of any tribo-film at the interface may influence the aforementioned processes. This current research uses reciprocating tribocorrosion tests of CoCrMo surfaces in saline, protein, and protein-free cell culture medium lubricants (0.9% NaCl, 25% Foetal Bovine Serum (FBS) diluted in Phosphate Buffered Saline (PBS), Dulbecco's Modified Eagle Medium (DMEM) and 25% FBS in DMEM solutions). Results show the addition of organic constituents give a better tribology and corrosion performances. XPS confirmed that chemical reactions happened on the tested surfaces. Calcium, phosphorus and sulphur are shown to be catalysed to react in tribology-induced processes and have important roles in tribocorrosion. These results contribute to the understanding of protein-metal interactions occurring in tribofilm formation on wearing surfaces.

1. Introduction

The use of CoCrMo alloy in orthopedic applications is widespread and usually the material of choice for load bearing tribological surfaces. For most Total Hip Replacements (THR) there are at least 1 or 2 metallic components where tribocorrosion processes may occur [1]. Whilst the use of Metal-on-Metal (MoM) implants has decreased to 10% of all newly implanted materials in the United Kingdom, for some cases (younger more active patients) there is still a desire for large diameter MoM devices. Metal-on-Metal (MoM) configurations were introduced as an alternative hip prostheses to address the problem of polymer debris and were initially regarded as less harmful to the human body [2]. However the issues associated with the release of Co and Cr metallic ions and debris due to tribocorrosion into the biological environment have raised concerns over the suitability of the material for biomedical applications. The applied metal alloys are mainly based on titanium, cobalt, iron, which has the distinguished passive corrosion behavior since an oxide film that develops at the surface spontaneously [3]. However, wear debris and release of metal ions due to the damage of oxide film have become the focus of much research due to extensive reported problems with some MoM devices [4].

CoCrMo alloys are regarded as the most suitable metal-based materials for load bearing tribological surfaces commonly found in hip joint replacements [5,6] owing to their excellent mechanical and corrosion properties. CoCrMo alloys are typically reported to have an elastic modulus around 200–220 GPa and hardness of approximately 40–50 HRC and therefore excellent in terms of low mechanical deformation and high wear resistance when compared to other common biomaterials such as Fe and Ti-based alloys [7]. CoCrMo alloys are reliable in their self-mating ability and have a better biocompatibility than other metal alloys [8]. However, several studies have shown that there are unanticipated levels of failure caused by wear and corrosion, of course being highlighted by the clinical community and orthopedic industries [9].

The fundamental mechanisms of wear and corrosion are recognized to solve the longevity problem of the orthopedic implants, however struggled to achieve due to the complex working environment [3,10]. There are complex compounds of metal and protein at the sliding contact zone which are generated due to the presence of frictional force and/or chemical interactions [11]. Ultimately, the effect of this extremely complex synovial fluid on joint replacement materials is a main concern.

The tribo-chemical reactions in the THR system occur when the protein from synovial fluid interacts with the tribo-activated surfaces, which eventually generate a tribochemical film termed as the tribofilm or tribo-material [12]. It has been hypothesized by some authors that this material formed may be beneficial in reducing the coefficient of friction and magnitudes of degradation at contacting interfaces. In some research, synovial fluid has been replicated by protein serum solution [13,14]. The complex metal-protein interactions are traced by the deposition of proteinaceous constituents on the metal surface, degradation products compositions or presence in the bulk lubricant [11].

* Corresponding author.
E-mail address: mnmt@leeds.ac.uk (M. Taufiqurrakhman).

https://doi.org/10.1016/j.biotri.2019.100104
Received 5 April 2019; Received in revised form 18 July 2019; Accepted 26 July 2019
Available online 27 July 2019

Several in-vitro works [15–17] consistently address the presence of carbonaceous formation while the other in-vivo studies [18,19] show oxide films and organic deposition at the worn surface. Espallargas et al. [3] categorized the possibility of the tribofilm features based on some published results. There are three different surface depositions can be summarized: thick passive oxide film on the metal surface, organic constituents cover metal surface without transitional oxide film and a thinner oxide film cover the metal surface with a high concentration of organic formation.

In general, the mechanisms of tribochemical reactions are influenced by many parameters such as contact pressure [20,21], sliding speed [14,20,22], sliding distance [22], lubricant constituents [23,24], rubbing cycle [25], and surface materials [21,24,26]. The following literatures have investigated how the organic species and surrounding environment build the tribofilm formation. Hesketh et al. [27] conducted a hip simulator tribocorrosion study to see the structure and chemical nature of tribofilm formed in MoM THRs. It found that the deposited particles within the film have a smooth and small size, containing cobalt sulphide, carbon and oxygen. It was hypothesized that the film contained decomposed proteins because of the high pressures between the contact points of the metal bearings [15,28]. Certainly, the reaction depends on the chemical composition of the materials and lubricants used. Yan et al. [24] found that the film formed in the MoM configuration was a complex nano-scale structured layer, generated by the tribochemical reaction between biological substances, such as protein and organics with the contact zone. The layer comprises the organic deposits of embedded particles [13,28]. The processes to create tribofilms in sliding conditions, which give solid lubricant properties and a protective effect as stated by Liao et al. [29] are not understood yet. Proteins have very complex chemical bonding, and they are susceptible to react if they unfold [30].

The adsorbed protein species have been shown to affect the corrosion/electrochemical processes of CoCrMo alloys [3]. Munoz and Mischler [31–33] investigated the roles of protein adsorption roles on the electrochemical properties of CoCrMo. It was observed that organic species, such as proteins tend to increase the corrosion rate of the alloy. This was explained by binding and transporting processes of protein and metal ion complexes away from solution-material interface. However, other studies [24,34] illustrated that the protein adsorption considerably enhances the corrosion resistance of the metal surfaces. The proteinaceous layer limits the access of oxygen to the material surfaces and this in turn then changes the anodic and cathodic reactions. A decreased corrosion rate occurs [35,36]. The rate of protein adsorption is electrochemically affected by the potential condition such as passive, transpassive and cathodic [31,37,38], while this study only works at OCP condition.

The fundamental mechanisms of wear and corrosion are recognized as one of the primary factors to overcome to ensure the longevity of the orthopedic implants. However, to date, engineers have struggled to achieve optimal performance due to the complex nature working environment not being fully understood [3,10]. The aim of this study was to investigate the tribo-chemical interactions between organic matter containing lubricants and their interactions with a CoCrMo alloy surface under tribocorrosion conditions. Tribocorrosion of CoCrMo was simulated using a pin-on-plate tribometer and the resultant tribofilms formed on the CoCrMo surface comparing in several lubricants: saline, protein serum-containing solution, protein-free cell culture medium solution (DMEM) and mixed protein-DMEM solution. The structure of the tribofilm on CoCrMo alloys was assessed by X-ray Photoelectron Spectroscopy (XPS) and how the film formation influences the tribocorrosion has been discussed.

2. Material and Methodology

2.1. Material Preparation

A reciprocating pin-on-plate tribometer was used to simulate tribocorrosion. The contact configuration comprised of a sphere on flat geometry, an alumina ball (Ø = 12 mm ± 0.76 μm) directly in contact with a flat low-carbon CoCrMo plate (Ø = 22 × 6 mm). The ball made of Al2O3 ceramic was manufactured by Atlas Ball and Bearing Company with grading standard of 25. The plate was made of Co-28Cr-6Mo alloy as standardized in ASTM F75–12 [39]. CoCrMo samples were cut from wrought bar stock to have 6 mm thickness and polished to Ra ~ 10 nm.

Four different types of lubricant were used:

- 0.9% NaCl solution (saline) – organic species-free
- 25% Foetal Bovine Serum (FBS) solution – protein contained
- Dulbecco's Modified Eagle Medium (DMEM) solution – protein-free cell culture medium
- 25% FBS in DMEM – to identify the mixed composition influence

Table 1 shows general characteristics of all testing lubricants as given by the supplier. The serum solution was made by 25% FBS mixed with deionized water, PBS (Phosphate Buffered Saline) diluted for the conductivity, and 0.03% sodium azide to avoid the growth of bacteria or any microorganisms. The FBS solution, as shown in Table 2, was produced by Sera Laboratories International with European grade and triple 0.1 μM sterile filtered. This serum mixture was used as the replication of protein present in the synovial joint fluid, with 25% FBS or has the same of minimum protein content 17 g/L. The serum solution has pH 7.4 and viscosity of > 0.001 Pa.s [40,41]. The Gibco's high-glucose DMEM solution in Table 3, manufactured by Thermo Fisher Scientific contains no protein, lipids, or any growth factors. DMEM contains Mg ions from magnesium sulfate ($MgSO_4$-$7H_2O$) which serum and NaCl solution do not. However, this solution has a high glucose of 4.5 mg/mL and concentration of amino acids, vitamins, and inorganic salts. In addition, this solution has pH 7.2, conductivity of 0.68 mS/cm, and commonly used for cell culture processing applications. This solution contains the same amount of chloride as the bovine serum solution, which will influence the corrosion behaviour. The saline solution has a viscosity of 0.000885 Pa.s [42].

2.2. Tribocorrosion Tests

A 3-electrode electrochemical cell was integrated into the tribometer and connected to a computer-controlled potentiostat, as seen in Fig. 1. The initial mean Hertzian contact pressure was P_{mean} of 815 MPa as the normal load of 30 N was constantly applied over time to the Al_2O_3 ball [27]. All tests were conducted with a sliding speed of 20 mm/s and temperature of 25 °C to observe the reaction in room temperature conditions. To explore the behaviour of tribology and corrosion current, the wear tests were conducted at Open Circuit Potential (OCP). In this particular condition, both the anodic and cathodic reaction rates are equal. Fig. 2 illustrates the tribocorrosion test

Table 1
Characteristics of the testing lubricants.

	0.9% NaCl	25% Bovine serum in PBS	DMEM	25% Bovine serum in DMEM
pH	6.9	7.4	7.2	7.2
Conductivity (mS/cm)	3.8	3.8	0.68	0.68
Viscosity (mPa s)	0.88	< 1	1.07	1.07
Lambda ratio λ	0.019	0.021	0.022	0.022
Protein (albumin, globulins)	0 g/L	17 g/L	0 g/L	17 g/L

Table 2
Foetal bovine serum compositions.

Foetal bovine serum	mg/L
ALAT (SGPT) Alanine transaminase	7 IU/L
ALP Alkaline Phosphatase	372 IU/L
ASAT (SGOT) Aspartate transaminase	38 IU/L
Gamma-Glutamyl Transferase	7 IU/L
Lactate Dehydrogenase	621 IU/L
Bilirubin ($C_{33}H_{36}N_4O_6$)	20
Calcium	140
Cholesterol ($C_{27}H_{46}O$)	340
Creatinine ($C_4H_7N_3O$)	270
Chloride	3580
Glucose ($C_6H_{12}O_6$)	910
Iron	1.58
Phosphorus	97
Potassium	469
Sodium	3127
Triglycerides	660
Urea (CH_4N_2O)	420
Uric Acid ($C_5H_4N_4O_3$)	18
Albumin	15,800
Alpha-Globulins	11,000
Beta-Globulins	7600
Gamma-Globulins	400
Immunoglobulin IgG	130

Table 3
DMEM cell culture medium compositions.

Amino acids	mg/L
Glycine ($C_2H_5NO_2$)	30
L-Arginine hydrochloride ($C_6H_{15}ClN_4O_2$)	84
L-Cystine 2HCl ($C_6H_{14}Cl_2N_2O_4S_2$)	63
L-Histidine hydrochloride-H2O ($C_6H_{12}ClN_3O_3$)	42
L-Isoleucine ($C_6H_{13}NO_2$)	105
L-Leucine ($C_6H_{13}NO_2$)	105
L-Lysine hydrochloride ($C_6H_{15}ClN_2O_2$)	146
L-Methionine ($C_5H_{11}NO_2S$)	30
L-Phenylalanine ($C_9H_{11}NO_2$)	66
L-Serine ($C_3H_7NO_3$)	42
L-Threonine ($C_4H_9NO_3$)	95
L-Tryptophan ($C_{11}H_{12}N_2O_2$)	16
L-Tyrosine ($C_9H_{11}NO_3$)	72
L-Valine ($C_5H_{11}NO_2$)	94
Vitamins	mg/L
Choline chloride ($C_5H_{14}ClNO$)	4
D-Calcium pantothenate ($C_{18}H_{32}CaN_2O_{10}$)	4
Folic Acid ($C_{19}H_{19}N_7O_6$)	4
Niacinamide ($C_6H_6N_2O$)	4
Pyridoxine hydrochloride ($C_8H_{12}ClNO_3$)	4
Riboflavin ($C_{17}H_{20}N_4O_6$)	0.4
Thiamine hydrochloride ($C_{12}H_{18}Cl_2N_4OS$)	4
i-Inositol ($C_6H_{12}O_6$)	7.2
Inorganic Salts	mg/L
Calcium Chloride ($CaCl_2$-$2H_2O$)	264
Ferric Nitrate ($Fe(NO_3)_3$"$9H_2O$)	0.1
Magnesium Sulfate ($MgSO_4$-$7H_2O$)	200
Potassium Chloride (KCl)	400
Sodium Bicarbonate ($NaHCO_3$)	3700
Sodium Chloride (NaCl)	6400
Sodium Phosphate monobasic (NaH_2PO_4-$2H_2O$)	141
Other Components	mg/L
D-Glucose (Dextrose) ($C_6H_{12}O_6$)	4500
Phenol Red ($C_{19}H_{14}O_5S$)	15
Sodium Pyruvate ($C_3H_3NaO_3$)	110

protocol. The OCP was measured in static conditions for 500 s to make sure the passivation becomes stable. Two hours of pure sliding test was then done while simultaneously measuring the average of friction values. To monitor the corrosion rate of CoCrMo in lubricants, Linear Polarization Resistance (LPR) was taken at 30 min intervals during the sliding condition. The potential was shifted −25 mV to +25 mV vs OCP

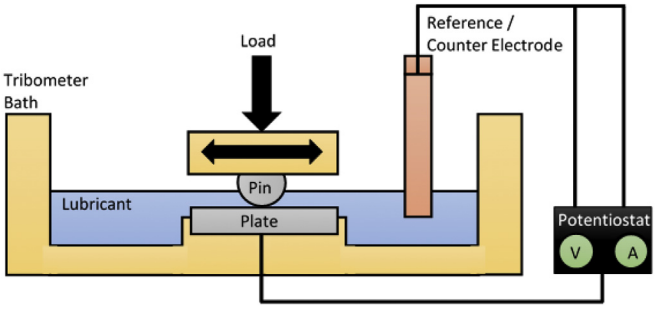

Fig. 1. Instrumented tribometer scheme.

at a scan rate of 0.25 mV/s. The measured current as a function of applied potential was plotted and the trend slope represented the polarization resistance (R_p). The obtained R_p is then converted into a corrosion current (I_{corr}) by using the Stern-Geary equation [43]. The tests were carried in all lubricants with three times repetition. All samples were taken out and stored in a desiccator.

2.3. Surface Analysis

Vertical scanning interferometry was conducted using an NPFlex (Bruker, USA) to obtain sample surface profiles as 3D images. The White Light Interferometry (WLI) used a magnification lens of 10×. The results from WLI scan were proceed by the Vision64 software (Bruker, USA), which can generate the 3D topography images. The topography images allow the wear scar contour and volume to be calculated after the appropriate removal of surface form and filter. The natural volume was measured by adjusting the layer height, so that the value below the plane was considered.

Scanning Electron Microscopy (SEM) using an EVO MA 15 (Carl Zeiss, Germany) aimed to observe the wear scar. The surface chemistry was interpreted by the results of X-ray Photoelectron Spectroscopy (XPS). XPS measurements were made inside and outside the wear scar of all surfaces. By using a Ta_2O_5 standard, the XPS etched 9 nm of surface depth per 10 s. The XPS produced element peaks that observe the chemical bonding reactions as a result of tribocorrosion tests. CasaXPS software supported the fitting processes before the peaks being interpreted in the proper region of binding energy (eV).

2.4. Statistical Analysis

To analyze the influence of proteinaceous constituents on tribology and corrosion current results, a one-way analysis of variance (ANOVA) was used. By input each testing lubricants (n = 3) as comparative groups, ANOVA test can determine if the friction coefficient, total volume loss and current density varied significantly for the presence of protein under sliding test. The level of significance used $\alpha = 0.05$ to be compared with p-value, which indicate whether each group was significantly different (p-value < 0.05) or not (p-value > 0.05).

3. Results and Discussion

3.1. Tribocorrosion Results

Fig. 3 shows the average coefficient of friction obtained for CoCrMo-alumina tribocorrosion contacts after 2-hours of sliding. Solutions containing DMEM has the lowest friction coefficient average followed by 25% serum in PBS samples. The coefficient of friction in Table 4, was seen to be significantly lower for surfaces slid in lubricants containing organic species ($p < 0.05$). No significant difference was seen in the coefficient of friction for lubricants containing organic species.

Fig. 4 shows the total volume loss and 2D cross-sectional traces of the areas subjected to sliding for the CoCrMo surface. It can be seen that

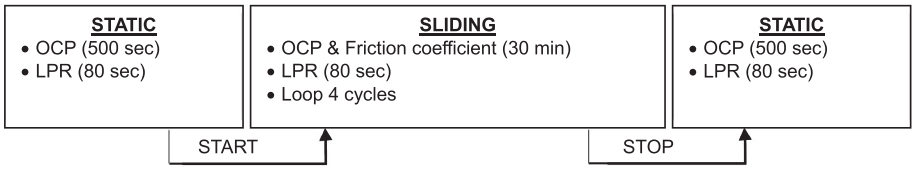

Fig. 2. Schematic of tribocorrosion tests protocol.

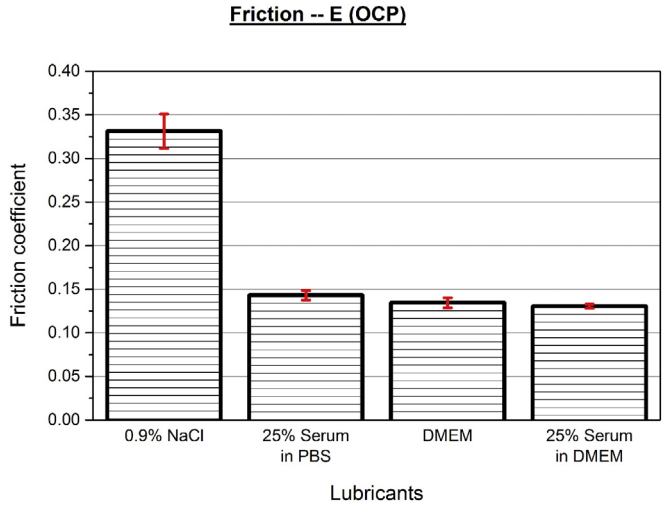

Fig. 3. The average and standard deviation of friction coefficient in all solution over the 2-h tests at 25 °C.

both measurements are in good agreement. The CoCrMo in NaCl has the highest wear volume of 0.0065 mm^3, followed by specimens in 25% serum in PBS and DMEM respectively for 2-hour tests. The results show the higher friction coefficient, wider scar and higher volume loss without the presence of proteinaceous substances. The presence of 25% serum in DMEM does not cause any significant changes to the friction and wear behaviour compared to the results in pure DMEM.

Fig. 5 shows the corrosion current density against test cycles and the averages of sliding current density measured by LPR in all solution over the 2-hour tests at 25 °C. Fig. 5a shows that upon the initiation of sliding, an increase in corrosion current density (exposed diameter of 25 mm) was observed. Fig. 5a summarized the average corrosion currents measured during sliding. The CoCrMo in 25% serum in PBS has the lowest corrosion current, followed by the samples in DMEM and NaCl respectively. The 25% serum presence in DMEM reduces the corrosion current compared to the average in pure DMEM. The result indicates the proteinaceous constituents have a significant effect on the corrosion behaviour in a tribocorrosion environment. This result may be influenced by the solution conductivity since the salt compositions are different.

Table 4 summarized the statistical approach by using analysis of variance (ANOVA) test. ANOVA tests were conducted between 2 groups of all tested lubricants used. Since the p-value is compared to the level of significance conducted in this study ($\alpha = 0.05$), some of them show a significant different (green columns) of averages in volume loss, friction and corrosion current.

The presence of protein serum and DMEM significantly affect the friction coefficient in the saline solution. The addition of 25% protein serum in DMEM does not have any significant effect on the volume loss compared to in the pure DMEM. The remaining volume loss ANOVA groups show the p-value is below 0.05. All of the group shows a significant difference of corrosion current density, as all p-value from the ANOVA < 0.05.

3.2. Surface Analysis

Scanning electron microscopy images of the CoCrMo surfaces after tribocorrosion are shown in Fig. 6. The key observations can be summarized as follows:

- The widest wear scar can be found on the NaCl sample; a massive abrasion occured
- Grooves have formed inside the wear scar of the serum samples, typically abrasive mechanisms
- A clear indication of film covered on the sample surface in serum solution and DMEM samples.
- The presence of 25% serum in DMEM does not have any significant effect to the wear behaviour compared to the results in pure DMEM.

Results above are in line with finding from some previous research [44–47]. Catelas et al. [45] stated that abrasive wear played a main role in MoM THRs failure and surgical revision and is in line with the wear mechanisms seen in Fig. 6. The mechanism could be hypothesized that debris generated from the surfaces will act as a third body in 25% serum solution. The third body effect describes as abrasive wear mechanism. The aggregated proteins became the third body within the configuration. Proteinaceous constituents formed a barrier to reduce material removal rate during tribological movement by interacting with the metal surface. As a boundary lubricant, the layers cover large surface areas then act in affecting adhesive and abrasive wear [18]. Mathew

Table 4
Analysis of variance (ANOVA) test.

Tested groups	Analysis of Variance Test (α = 0.05)		
	Friction coefficient ANOVA (p-value)	Volume loss ANOVA (p-value)	Current density ANOVA (p-value)
0.9% NaCl -- 25% Serum in PBS	9.34E-05	0.0079	5.56E-09
0.9% NaCl -- DMEM	7.86E-05	0.0015	9.88E-07
0.9% NaCl -- 25% Serum in DMEM	6.43E-05	0.0015	1.28E-08
25% Serum in PBS -- DMEM	0.1323	0.0063	1.89E-05
25% Serum in PBS -- 25% Serum in DMEM	0.0739	0.0059	9.00E-04
DMEM -- 25% Serum in DMEM	0.3453	0.6593	1.20E-04

p-value < α 0.05 (Significantly different)
p-value > α 0.05 (Not significantly different)

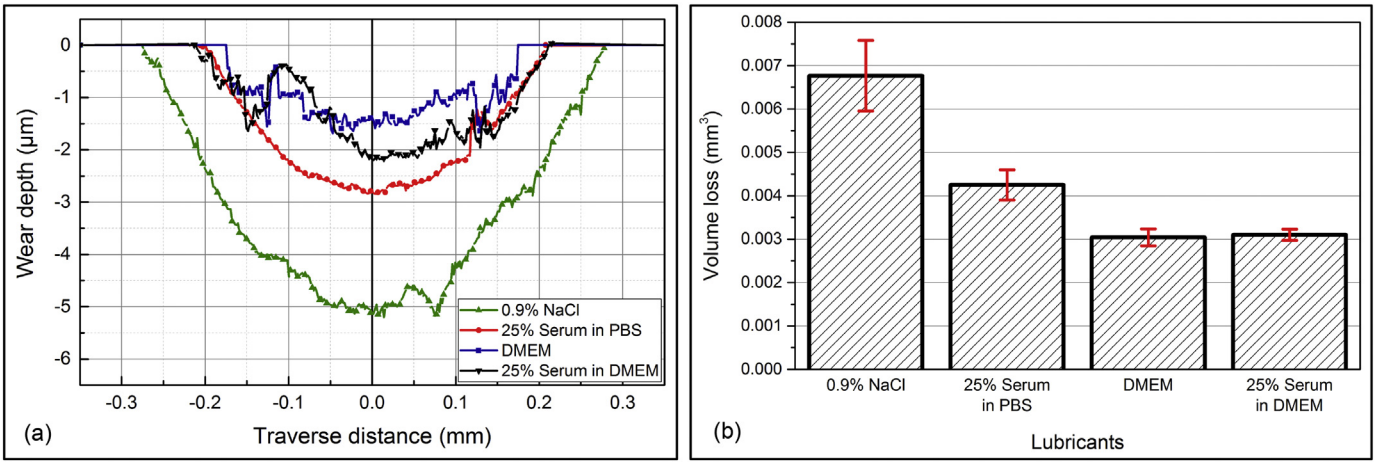

Fig. 4. The comparison of (a) cross-section wear and (b) volume loss (average and standard deviation for error bars) CoCrMo in all solution over the 2-hour tests at 25 °C.

et al. [48] observed that the presence of protein resulted in a 23% decrease of the total volume loss in a CoCr disc. It was assumed that the total volume loss has a similar trend with the friction coefficient average.

3.3. Surface Chemistry Analysis

The tribocorrosion results are closely linked to the nature of the lubricant used for testing. As seen in the previous sections, the solution containing organic constituents has a better lubricating effect, indicated by reduced coefficient of friction and wear volume, when compared to samples slid in a saline environment. The role of the tribofilm is extremely important and XPS has been used to evaluate the nature of the film.

3.3.1. The Characteristics of Surface Film

Fig. 7 shows the elemental composition (as atomic%) as a function of depth determined by XPS analysis both inside and outside the wear scar. The graphs present cross-sectional views of the film composition, from the very top to approximately 90 nm in depth. An oxide presence on the wear scar of NaCl samples (Fig. 7b) has the thickness of ~27 nm, which was thicker than the outside of the worn section. A proteinaceous film with the thickness of 45 nm deposited on the wear scar of serum samples (Fig. 7d), which is dominated by the carbon and phosphorus. Sulphur is dominant on the wear scar of DMEM samples (Fig. 7f and g). The presence of 25% serum in DMEM enhances the carbon percentages. Cobalt (Co 2p peaks), chromium (Cr 2p peaks), and molybdenum (Mo 3d peaks) increase through the layers since they are covered by the film [49,50].

It is clear that there is no carbon or any proteinaceous species deposited on the NaCl samples as expected. In serum, there is carbon, nitrogen and phosphorus on the sample surface at high concentrations. This is because the serum dominantly comprises of proteins such as albumin, globulins, uric acid, urea, triglycerides, bilirubin and creatinine [51]. In DMEM, the carbon percentage of the tribofilm is less than the proteinaceous constituents such as sulphur, phosphorus, and calcium. Magnesium can be seen in DMEM-contained solutions, since DMEM comprises magnesium sulfate ($MgSO_4$-$7H_2O$) as one of the inorganic salts.

By comparing the atomic percentages, this may prove that some of the proteinaceous-metal complexations are tribology induced [52,53]. It suggests that some proteinaceous substances need to be in the tribological condition to be activated. Fig. 8 shows that the Ca 2p and P 2p peaks have a higher concentration inside the wear track. The C 1 s, O 1 s and proteinaceous constituents are also much stronger on the inside compared to the outside of wear scar. The serum solution contains calcium, albumin and alpha, beta and gamma-globulin which have a native protein structure [51]. The native protein is mostly constructed by carbon, nitrogen, oxygen, hydrogen, phosphorus and chains of disulfide. Furthermore, the unfolded protein can adsorb into the metal

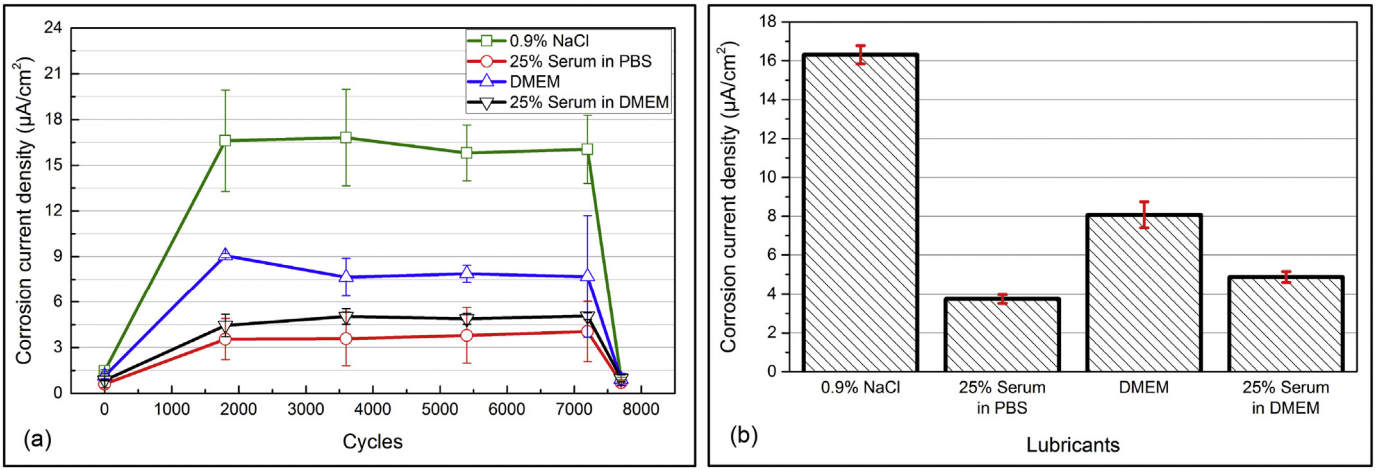

Fig. 5. (a) The corrosion current density vs cycles and (b) averages (bars) and standard deviation (error bars) of sliding current density measured by LPR over the 2-hour tests at 25 °C.

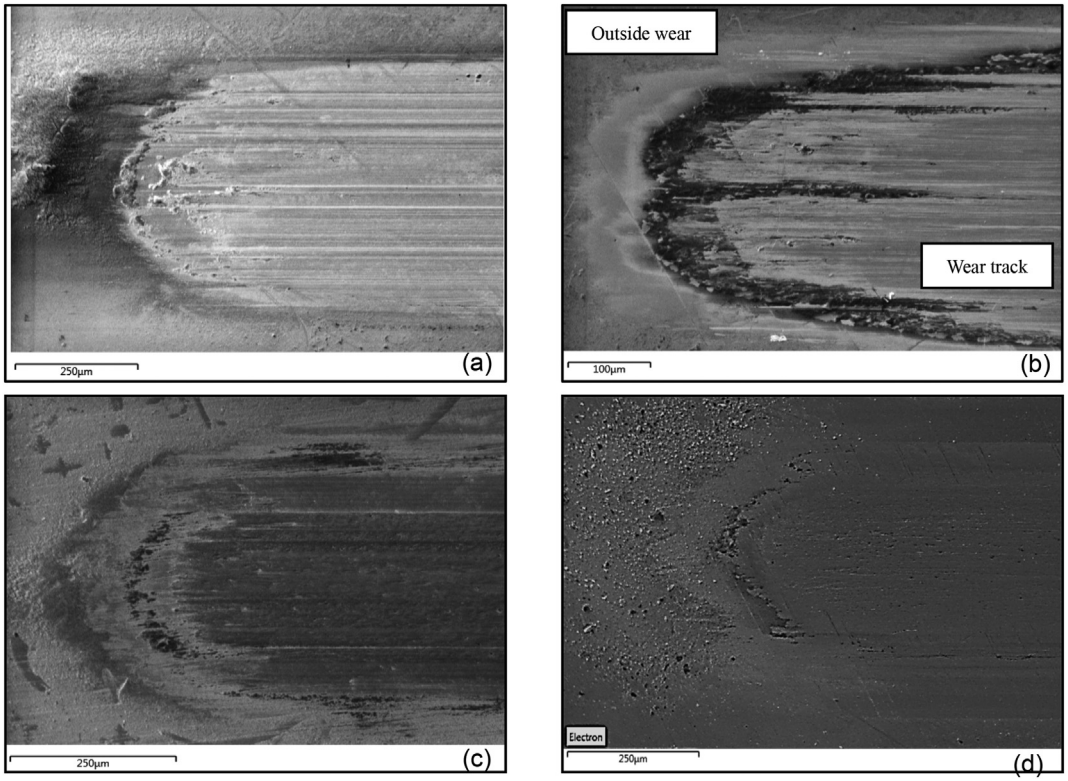

Fig. 6. SEM images of wear track of CoCrMo in (a) 0.9% NaCl, (b) 25% serum in PBS, (c) DMEM and (d) 25% serum in DMEM solution over the 2-hour tests at 25 °C.

surface and become easier to react with the oxide and metal ions. A larger ratio between Ca 2p inside and outside wear suggested that the DMEM is more reactive than serum since it already contains sulphur, amino acids and other minerals with protein-free.

3.3.2. Chemical Compounds of Metal-Proteinaceous Interaction

There are a number of tribo-chemical pathways that exist that may result in the formation of a tribo-film. However, without a thorough understanding of chemical speciation of the tribo-films formed, the route to formation cannot be determined. Fig. 9 shows deconvolution of the carbon peaks (C 1 s) obtained at the binding energy range of 280–292 eV. These could be fitted into five different peaks (~282.4 eV, 284.5 eV, 286.3 eV, 288.2 eV, 289.2 eV as in Fig. 9). Some organic compounds were bond metal ions and hydro-oxide elements [54].

The Ca 2p on both serum and DMEM samples, as shown in Fig. 8, has two different peaks as the orbital split with the Ca 2p 3/2 binding energy of ~347.30 eV [55]. It is assumed that the calcium binds the other elements such as calcium oxide (CaO), calcium hydroxide ($Ca(OH)_2$) and calcium carbonate ($CaCO_3$) with the binding energy of O 1 s and C 1 s are ~531.50 eV [56] and ~289.20 eV [57] respectively. The calcium hydrogen phosphate ($CaHPO_4$) also appear on the XPS peaks interpretations as the P 2p 3/2 has the binding energy of ~133.30 eV [57].

A strong phosphorus (P 2p) signal is detected inside the wear scar tested in 25% serum diluted PBS. Chromium phosphate ($CrPO_4$) appears on the CoCrMo specimens generated in both serum and DMEM containing solutions. The P 2p 3/2 shows a binding energy of ~133.40 eV [58] along with the Cr 2p 3/2 at ~577.80 eV [59]. $CrPO_4$ was found in some previous research as a corrosion product on MoM components [60]. Cooper et al. [61] observed that some amounts of chromium phosphate particles were seen within fibrin and in the tissue covering the joint surface.

Fig. 10 shows XPS comparison of Co 2p, Cr 2p and Mo 3d peaks inside the wear scar in all lubricants. The Co 2p signal indicated peaks arising at 781.18 eV and 788.00 eV indicating the existence of CoO and Co-satellite respectively [11,62]. The areas of CoO and Co-satellite spectra grow significantly in the presence of serum. The signal on DMEM sample tends to be similar with the pre-tested sample. The oxide (O 1 s) mostly represents the metal-oxide film which is formed by the passivation processes [49,63,64].

The Cr 2p signal indicated the debris of $Cr(OH)_3$ and Cr_2O_3 with peaks at 577.50 eV and 576.28 eV respectively [11,62,65,66]. The comparison observed that a higher ratio of oxide in Cr 2p peaks are found in serum containing lubricants.

The Mo 3d spectra shows that the sulphur is identified at ~227.00 eV on the sample in organic-contained solutions. DMEM result has a higher concentration of sulphur bond with the molybdenum compared to the 25% serum in PBS. MoO_2 and MoO_3 are resolved at 229.50 eV and 233.10 eV respectively [11,62]. The peaks observed that the MoO_2 and MoO_3 have a stronger concentration in the presence of serum. All comparison suggested that the serum presence can enhance the rate of oxide-metal bonding reaction.

3.4. The Influence of Film Formation on the Tribo-Corrosion Aspects

The coefficient of friction was lower in the presence of organic containing solutions, which has been proved statistically by ANOVA test. In the saline sample, it is only the passive oxide film covering the metal surface as the protection. The passive film is removed after rubbing. Although the repassivation process can reform the film, it takes some time to oxidize the metal ion and have a stable reformation on the surfaces [67]. In the solutions containing serum and DMEM, proteinaceous constituents play a very important role in constructing the tribofilm. Proteins bind the metal ions which precipitate on the surface as a biofilm.

Total volume loss is lower for a DMEM containing solution. Amino acids and proteinaceous species in DMEM act as a more reactive species on the surface. It has a lower friction and wear than serum and also a sulphur-rich layer is deposited on the substrate surface. There is an indication about the effect of sulphur concentrations in Mo3d peak with

Reference sample surface (a)

Signal peaks	Atomic percentage (%)
Co 2p	54.89
Cr 2p	32.80
Mo 3d	8.09
O 1s	4.22

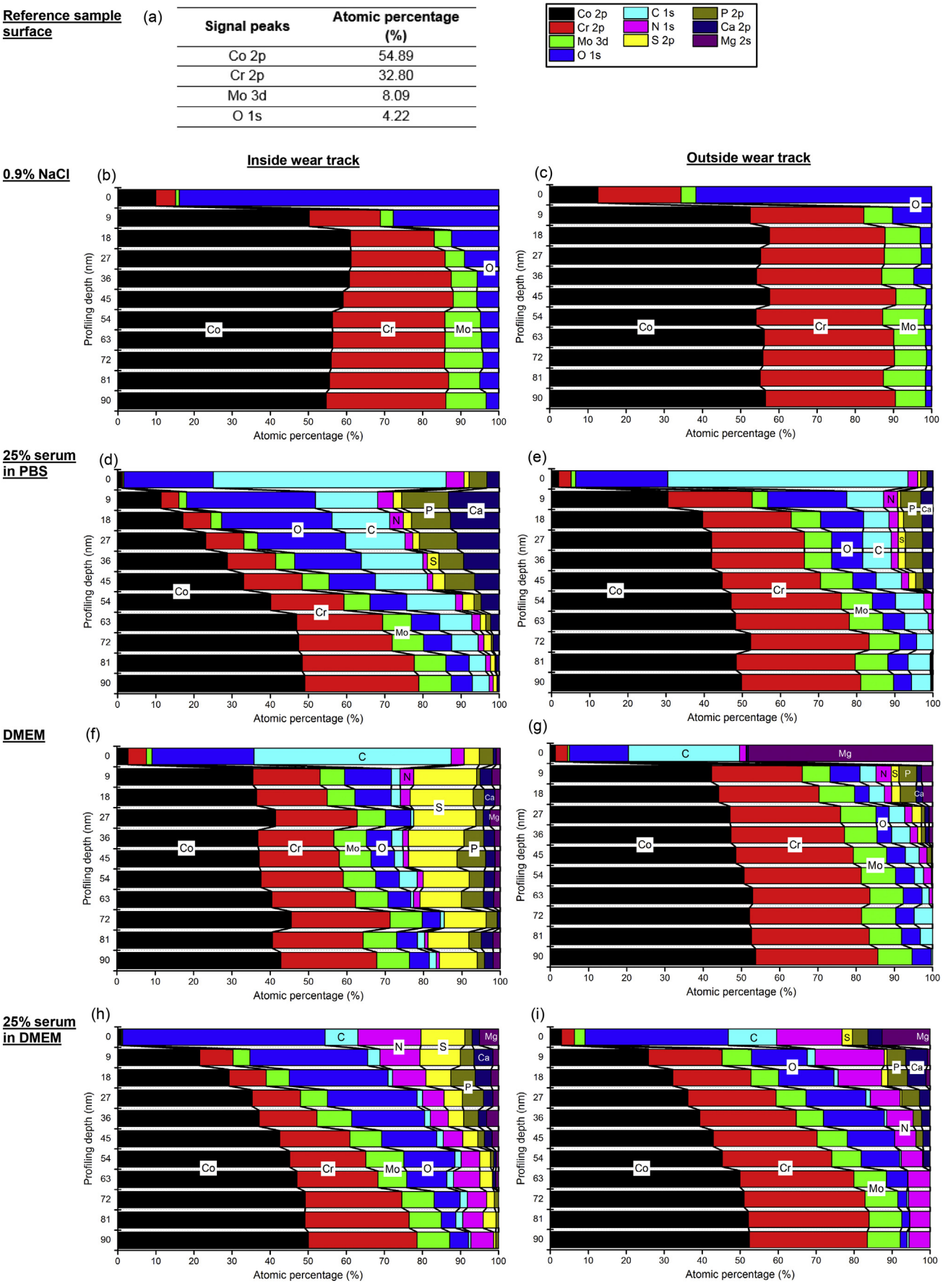

Fig. 7. XPS atomic concentration of (a) reference sample and from top surface to 90 nm depth profiling on both inside (all left side) and outside wear scar (all right side) of the tested samples in: (b and c) 0.9% NaCl, (d and e) 25% serum in PBS, (f and g) DMEM and (h and i) 25% serum in DMEM.

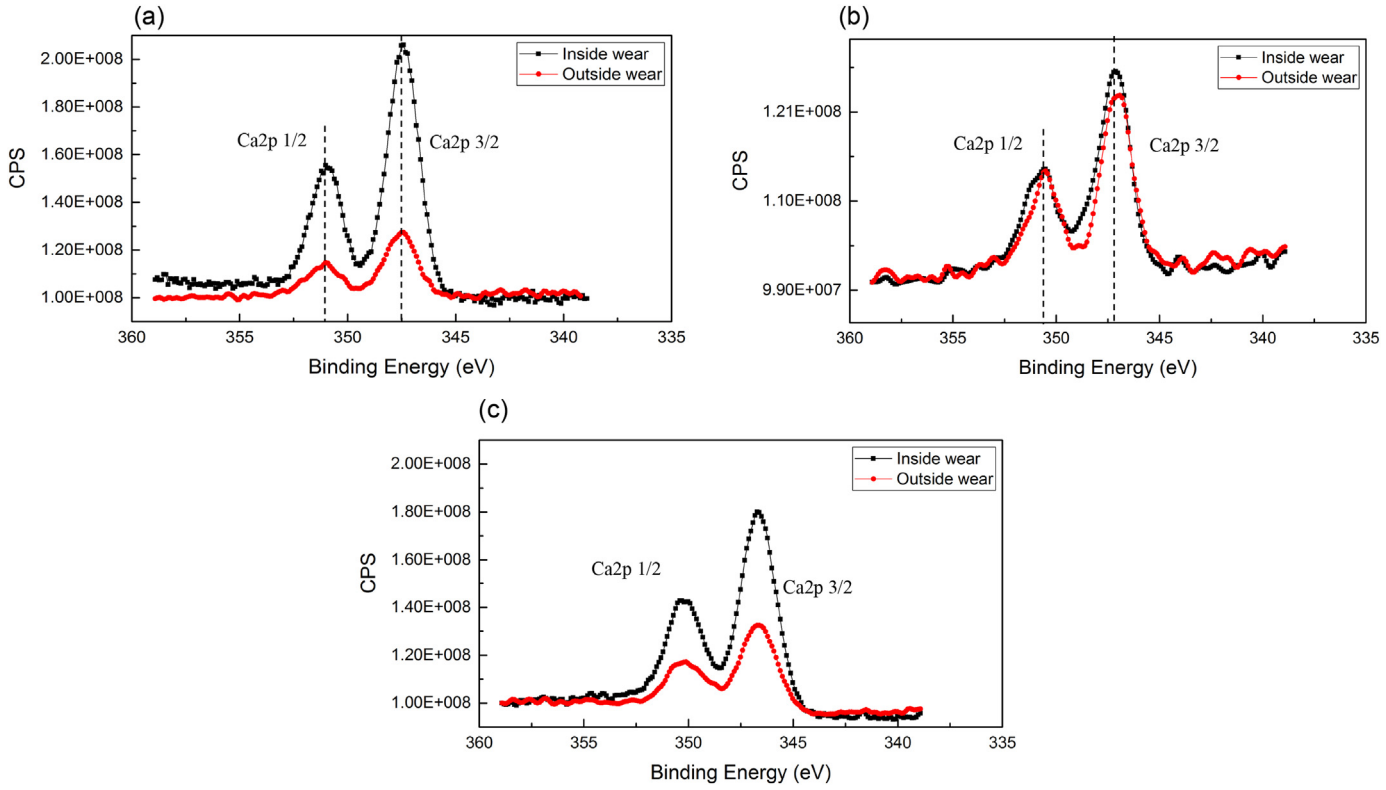

Fig. 8. XPS comparison of calcium (Ca 2p) peaks inside and outside the wear scar in (a) 25% serum in PBS, (b) pure DMEM and (c) 25% serum in DMEM.

the wear resistance. The presence of sulphur on the surface tends to reduce the wear volume loss [68,69]. This may be hypothesized as an important role to the tribology behaviour specifically in DMEM.

Samples of 25% serum in PBS have the higher wear volume loss but a lower corrosion current compared to the samples in pure DMEM. This trend is similar when 25% serum is added into the DMEM solution. As explained that the higher volume of surface material removed in 25% serum solution is caused by abrasive wear. The aggregated proteins act as the 3rd body within the configuration contribute to the abrasion mechanism. The abrasive also may be correlated to the oxide concentration that appear on the Co 2p, Cr 2p and Mo 3d peaks. As seen in the XPS figures, the presence of serum can increases the CoO, $Cr(OH)_3$, MoO_2 and MoO_3 ratio. The debris of these oxide film is hypothesized to enhance the abrasive wear in the serum and saline.

In this case, corrosion current is variable and not necessarily linked to high volume loss or friction coefficient. The trend is also influenced by the conductivity changes in each lubricant. However, the protein adsorption can inhibit the oxidation reaction in the tribological condition, therefore, the oxidation of metal ions is reduced. Lyvers et al. [70] obtained similar electrochemical results on CoCrMo substrates. The presence of protein substances reduced the charge transfer and suppressed the corrosion reaction on the exposed metal surface under mechanical wear. Protein substances assumed to enhance the corrosion resistance of CoCrMo surface. It assumed that the DMEM is more susceptible to be corroded as it contains reactive species such as high sulphur concentration.

The constituents from serum and DMEM solutions have their own role. The deposition of $CaHPO_4$ is suggested to play an important role related to the friction and wear decrease. The formation is caused by the reaction of organic substances which are affected by heat and pH conditions [71,72]. Zhang et al. [73] used the calcium phosphate as a coating on metal alloys or biomaterial implants and for osseous defect treatments. Those tribofilms give a robust lubrication effect while the surfaces against each other. The tribofilm behaviour eventually will change by the tribochemical reactions with the metal-organic interactions. Understanding the detailed mechanisms of lubricant-metal

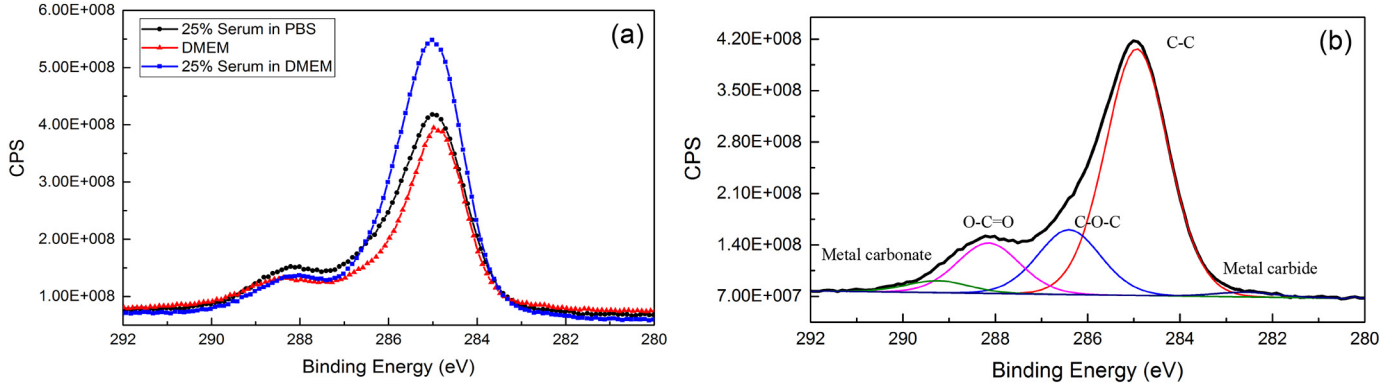

Fig. 9. Carbon C1s signals (a) comparison and (b) each peaks interpretation.

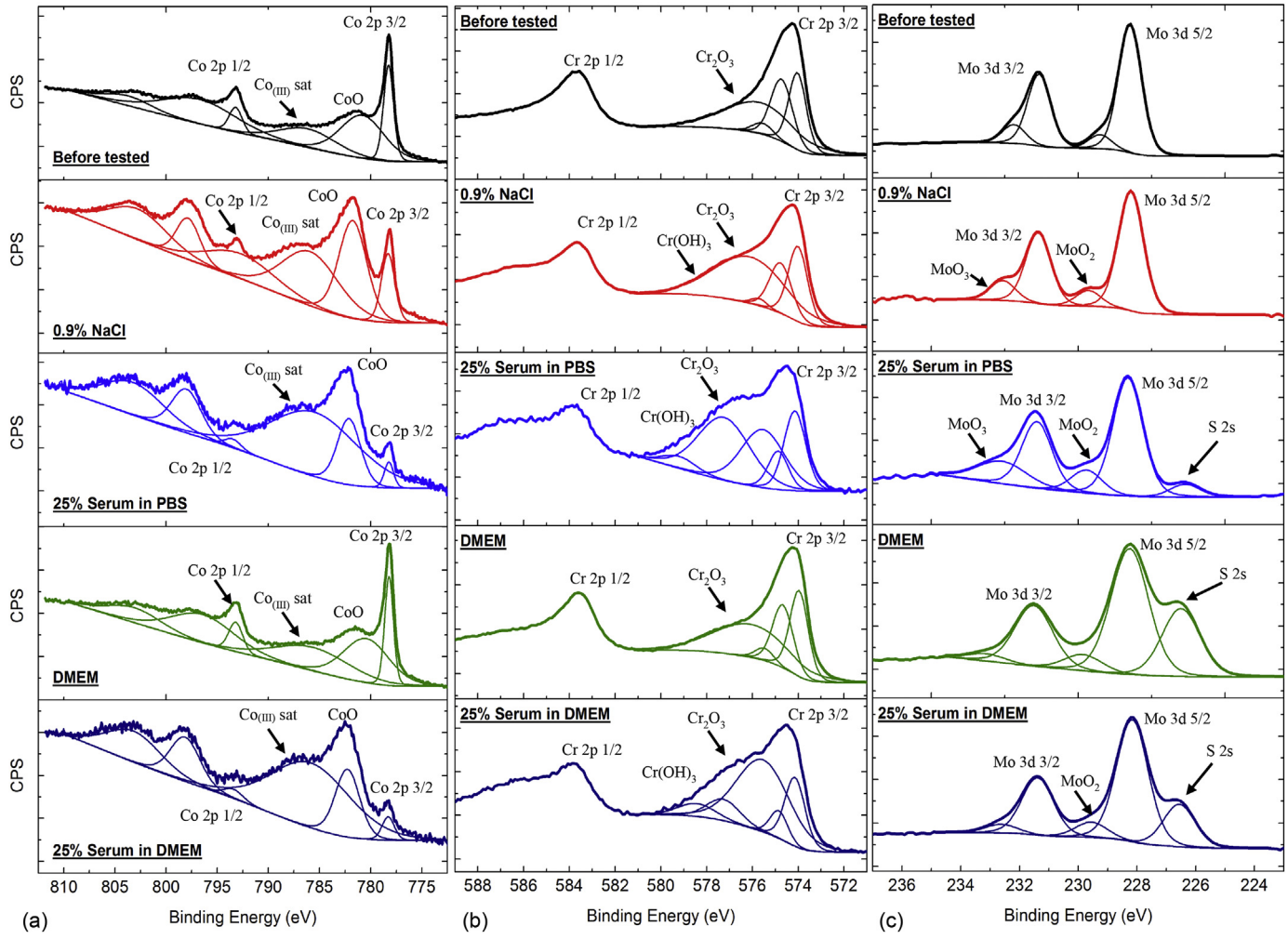

Fig. 10. XPS comparison of (a) Co 2p, (b) Cr 2p and (c) Mo 3d peaks inside the wear scar in all lubricants.

interaction in building the film is very important to do in the further research.

4. Conclusions

This paper has investigated that the differences of tribocorrosion behaviour are depended on the lubricant constituents. The phenomenon happened because of the different reactions of lubricant constituent which affect the tribofilm formation. The following points are concluded the study:

- The presence of protein serum and DMEM significantly affect the friction coefficient in the saline solution which has been proved by ANOVA test. The complex biofilm formation tends to give a better lubrication effect.
- Total volume loss is statistically proved to be lower in both DMEM-containing solutions. The hypothesis is that high sulphur species from DMEM (as indicated in Mo 3d XPS surface signal) tends to increase the wear resistance.
- The addition of 25% serum in DMEM can enhances the corrosion resistance but reduces the wear performance. SEM image shows a massive abrasive wear mechanism inside the wear track of samples in the serum-containing solution.
- Some proteinaceous species such as calcium, phosphorus and sulphur are tribology-induced, which is proved by XPS profiling analysis.

Declaration of Competing Interest

The authors have no conflicts of interest to disclose.

Acknowledgement

The authors would like to thank all supports from Institute of Functional Surfaces, University of Leeds. The first author would also like to thank LPDP (Indonesia Endowment Fund for Education) for the support given during his study.

References

[1] National Joint Registry 14th Annual Report 2017, National Joint Registry, 2017.
[2] P. Grigoris, P. Roberts, K. Panousis, The development of the DuromTM metal-on-metal hip resurfacing, Hip Inter. 16 (Suppl. 4) (2006) 65–72.
[3] N. Espallargas, A. Fischer, A. Igual Muñoz, S. Mischler, M.A. Wimmer, In-situ generated tribomaterial in metal/metal contacts: current understanding and future implications for implants, Biotribology 10 (2017) 42–50.
[4] A.R. Beadling, M. Bryant, D. Dowson, A. Neville, Tribocorrosion of hard-on-hard total hip replacements with metal and ceramic counterfaces under standard and adverse loading conditions, Tribol. Int. 103 (2016) 359–367.
[5] T.A. Simoes, M.G. Bryant, A.P. Brown, S.J. Milne, M. Ryan, A. Neville, et al., Evidence for the dissolution of molybdenum during tribocorrosion of CoCrMo hip implants in the presence of serum protein, Acta Biomater. 45 (2016) 410–418.
[6] S. Mischler, A.I. Muñoz, Wear of CoCrMo alloys used in metal-on-metal hip joints: a tribocorrosion appraisal, Wear 297 (2013) 1081–1094.
[7] 3T PRD, Material Specification: Cobalt Chrome Alloy Co28Cr6Mo, (2013).
[8] L. Kunčická, R. Kocich, T.C. Lowe, Advances in metals and alloys for joint replacement, Prog. Mater. Sci. 88 (2017) 232–280.
[9] D.J. Langton, S.S. Jameson, T.J. Joyce, N.J. Hallab, S. Natu, A.V. Nargol, Early failure of metal-on-metal bearings in hip resurfacing and large-diameter total hip

replacement: a consequence of excess wear, J. Bone Joint Surg. British Vol. 92 (2010) 38–46.
[10] J.J. Jacobs, J.L. Gilbert, R.M. Urban, Corrosion of metal orthopaedic implants, J. Bone Joint Surg. Am. 80 (1998) 268–282.
[11] I. Milosev, M. Remskar, In vivo production of nanosized metal wear debris formed by tribochemical reaction as confirmed by high-resolution TEM and XPS analyses, J. Biomed. Mater. Res. A 91 (2009) 1100–1110.
[12] S. Ghosh, D. Choudhury, T. Roy, A. Moradi, H.H. Masjuki, B. Pingguan-Murphy, Tribological performance of the biological components of synovial fluid in artificial joint implants, Sci. Technol. Adv. Mater. 16 (2015) 045002.
[13] J. Fan, C. Myant, R. Underwood, P. Cann, Synovial fluid lubrication of artificial joints: protein film formation and composition, Faraday Discuss. 156 (2012) 69–85.
[14] A. Mavraki, P.M. Cann, Friction and lubricant film thickness measurements on simulated synovial fluids, Proceed. Inst. Mech. Eng. Part J. 223 (2009) 325–335.
[15] M.A. Wimmer, J. Loos, R. Nassutt, M. Heitkemper, A. Fischer, The acting wear mechanisms on metal-on-metal hip joint bearings: in vitro results, Wear 250 (2001) 129–139.
[16] R. Pourzal, R. Theissmann, M. Morlock, A. Fischer, Micro-structural alterations within different areas of articulating surfaces of a metal-on-metal hip resurfacing system, Wear 267 (2009) 689–694.
[17] P. Zeng, A. Rana, R. Thompson, W.M. Rainforth, Subsurface characterisation of wear on mechanically polished and electro-polished biomedical grade CoCrMo, Wear 332–333 (2015) 650–661.
[18] M.A. Wimmer, C. Sprecher, R. Hauert, G. Tager, A. Fischer, Tribochemical reaction on metal-on-metal hip joint bearings - a comparison between in-vitro and in-vivo results, Wear 255 (2003) 1007–1014.
[19] Y. Liao, R. Pourzal, M.A. Wimmer, J.J. Jacobs, A. Fischer, L.D. Marks, Graphitic Tribological layers in metal-on-metal hip replacements, Science 334 (2011) 1687–1690.
[20] C. Myant, R. Underwood, J. Fan, P.M. Cann, Lubrication of metal-on-metal hip joints: the effect of protein content and load on film formation and wear, J. Mech. Behav. Biomed. Mater. 6 (2012) 30–40.
[21] Q.E. Meng, F. Liu, J. Fisher, Z.M. Jin, Contact mechanics and lubrication analyses of ceramic-on-metal total hip replacements, Tribol. Int. 63 (2013) 51–60.
[22] B. McEntire, R. Lakshminarayanan, D. Ray, I. Clarke, L. Puppulin, G. Pezzotti, Silicon nitride bearings for Total joint Arthroplasty, Lubricants 4 (2016) 35.
[23] D. Nečas, M. Vrbka, F. Urban, I. Křupka, M. Hartl, The effect of lubricant constituents on lubrication mechanisms in hip joint replacements, J. Mech. Behav. Biomed. Mater. 55 (2016) 295–307.
[24] Y. Yan, A. Neville, D. Dowson, Biotribocorrosion of CoCrMo orthopaedic implant materials - assessing the formation and effectof the biofilm, Tribol. Int. 40 (2007) 1492–1499.
[25] M. Vrbka, T. Návrat, I. Křupka, M. Hartl, P. Šperka, J. Gallo, Study of film formation in bovine serum lubricated contacts under rolling/sliding conditions, Proceed. Inst. Mech. Eng. Part J. 227 (2013) 459–475.
[26] J. Yang, J. Black, Competitive binding of chromium, cobalt and nickel to serum proteins, Biomaterials 15 (1994) 262–268.
[27] J.E.T. Hesketh, Tribocorrosion of Total Hip Replacements, Ph.D. Thesis University of Leeds, 2012.
[28] J. Hesketh, M. Ward, D. Dowson, A. Neville, The composition of tribofilms produced on metal-on-metal hip bearings, Biomaterials 35 (2014) 2113–2119.
[29] Y. Liao, E. Hoffman, M. Wimmer, A. Fischer, J. Jacobs, L. Marks, CoCrMo metal-on-metal hip replacements, Phys. Chem. Chem. Phys. 15 (2013), https://doi.org/10.1039/c2cp42968c.
[30] V.K. Maskiewicz, P.A. Williams, S.J. Prates, J.G. Bowsher, I.C. Clarke, Characterization of protein degradation in serum-based lubricants during simulation wear testing of metal-on-metal hip prostheses, J Biomed Mater Res B Appl Biomater 94 (2010) 429–440.
[31] A.I. Muñoz, S. Mischler, Electrochemical quartz crystal microbalance and X-Ray photoelectron spectroscopy study of cathodic reactions in bovine serum albumin containing solutions on a physical vapour deposition-CoCrMo biomedical alloy, Electrochim. Acta 180 (2015) 96–103.
[32] A.I. Muñoz, S. Mischler, Interactive effects of albumin and phosphate ions on the corrosion of CoCrMo implant alloy, J. Electrochem. Soc. 154 (2007) C562–C570.
[33] A.I. Munoz, S. Mischler, Effect of the environment on wear ranking and corrosion of biomedical CoCrMo alloys, J. Mater. Sci. Mater. Med. 22 (2011) 437–450.
[34] D.F. Williams, I.N. Askill, R. Smith, Protein absorption and desorption phenomena on clean metal surfaces, J. Biomed. Mater. Res. 19 (1985) 313–320.
[35] B.D. Ratner, A.S. Hoffman, F.J. Schoen, J.E. Lemons, Biomaterials Science: An Introduction to Materials in Medicine, Academic press, 2004.
[36] F. Contu, B. Elsener, H. Bohni, Characterization of implant materials in fetal bovine serum and sodium sulfate by electrochemical impedance spectroscopy. II. Coarsely sandblasted samples, J. Biomed. Mater. Res. A 67 (2003) 246–254.
[37] S. Kerwell, D. Baer, E. Martin, Y.A. Liao, M. Wimmer, K. Shull, et al., Electrochemically Induced Film Formation on CoCrMo Alloy for Hip Implant Application, (2017).
[38] C. Valero-Vidal, A. Igual-Muñoz, C.-O. Olsson, S. Mischler, Adsorption of BSA on Passivated CoCrMo PVD alloy: an EQCM and XPS investigation, J. Electrochem. Soc. 161 (2014) C294–C301.
[39] ASTM International, ASTM F75–12, Standard Specification for Cobalt-28 Chromium-6 Molybdenum Alloy Castings and Casting Alloy for Surgical Implants (UNS R30075), West Conshohocken, PA (2012).
[40] International Organization for Standardization. ISO 14242-1:2002, Implants for Surgery – Wear of Total Hip-Joint Prostheses – Part 1: Loading and Displacement Parameters for Wear-Testing Machines and Corresponding Environmental Conditions for test, (2002).
[41] Y. Yan, Corrosion and Tribo-Corrosion Behaviour of Metallic Orthopaedic Implant Materials, Ph.D. Thesis University of Leeds, 2006.
[42] J. Kestin, H.E. Khalifa, R.J. Correia, Tables of the dynamic and kinematic viscosity of aqueous NaCl solutions in the temperature range 20–150 C and the pressure range 0.1–35 MPa, J. Phys. Chem. Ref. Data 10 (1981) 71–88.
[43] A.R. Beadling, Biotribocorrosion of Hard-on-Hard Bearing Surfaces in Orthopaedic Hip Replacements, Ph.D. Thesis University of Leeds, 2016.
[44] C.G. Figueiredo-Pina, Y. Yan, A. Neville, J. Fisher, Understanding the differences between the wear of metal-on-metal and ceramic-on-metal total hip replacements, Proc. Inst. Mech. Eng. H J. Eng. Med. 222 (2008) 285–296.
[45] I. Catelas, M.A. Wimmer, S. Utzschneider, Polyethylene and metal wear particles: characteristics and biological effects, Semin. Immunopathol. 33 (2011) 257–271.
[46] H. Ito, K. Kaneda, T. Yuhta, I. Nishimura, K. Yasuda, T. Matsuno, Reduction of polyethylene wear by concave dimples on the frictional surface in artificial hip joints, J. Arthroplast. 15 (2000) 332–338.
[47] R. Lee, A. Essner, A. Wang, W.L. Jaffe, Scratch and wear performance of prosthetic femoral head components against crosslinked UHMWPE sockets, Wear 267 (2009) 1915–1921.
[48] M.T. Mathew, J.J. Jacobs, M.A. Wimmer, Wear-corrosion synergism in a CoCrMo hip bearing alloy is influenced by proteins, Clin. Orthop. Relat. Res. 470 (2012) 3109–3117.
[49] R. Steinberger, C.E. Celedón, B. Bruckner, D. Roth, J. Duchoslav, M. Arndt, et al., Oxygen accumulation on metal surfaces investigated by XPS, AES and LEIS, an issue for sputter depth profiling under UHV conditions, Appl. Surf. Sci. 411 (2017) 189–196.
[50] M. Jenko, M. Gorenšek, M. Godec, M. Hodnik, B. Batič, Č. Donik, et al., Surface chemistry and microstructure of metallic biomaterials for hip and knee endoprostheses, Appl. Surf. Sci. 427 (2018) 584–593.
[51] Sera Laboratories International Ltd, Certificate of Analysis. Product: Foetal Bovine Serum European Grade. Colombia, (2017).
[52] S. Ray, A.G. Shard, Quantitative analysis of adsorbed proteins by X-ray photoelectron spectroscopy, Anal. Chem. 83 (2011) 8659–8666.
[53] E. Vanea, V. Simon, XPS study of protein adsorption onto nanocrystalline aluminosilicate microparticles, Appl. Surf. Sci. 257 (2011) 2346–2352.
[54] B.P. Payne, M.C. Biesinger, N.S. McIntyre, Use of oxygen/nickel ratios in the XPS characterisation of oxide phases on nickel metal and nickel alloy surfaces, J. Electron Spectrosc. Relat. Phenom. 185 (2012) 159–166.
[55] H. Van Doveren, J.A.T.H. Verhoeven, XPS spectra of Ca, Sr, Ba and their oxides, J. Electron Spectrosc. Relat. Phenom. 21 (1980) 265–273.
[56] T. Hanawa, M. Ota, Calcium phosphate naturally formed on titanium in electrolyte solution, Biomaterials 12 (1991) 767–774.
[57] B. Demri, D. Muster, XPS study of some calcium compounds, J. Mater. Process. Technol. 55 (1995) 311–314.
[58] I.M. Watson, J.A. Connor, R. Whyman, Non-crystalline chromium, molybdenum and tungsten phosphate films prepared by metal organic chemical vapour deposition, Thin Solid Films 201 (1991) 337–349.
[59] T.P. Moffat, R.M. Latanision, R.R. Ruf, An X-ray photoelectron spectroscopy study of chromium-metalloid alloys—III, Electrochim. Acta 40 (1995) 1723–1734.
[60] A. Di Laura, P.D. Quinn, V.C. Panagiotopoulou, H.S. Hothi, J. Henckel, J.J. Powell, et al., The chemical form of metal species released from corroded taper junctions of hip implants: synchrotron analysis of patient tissue, Sci. Rep. 7 (2017) 10952.
[61] H.J. Cooper, R.M. Urban, R.L. Wixson, R.M. Meneghini, J.J. Jacobs, Adverse local tissue reaction arising from corrosion at the femoral neck-body junction in a dual-taper stem with a cobalt-chromium modular neck, J. Bone Joint Surg. Am. 95 (2013) 865–872.
[62] I. Milošev, H.H. Strehblow, The composition of the surface passive film formed on CoCrMo alloy in simulated physiological solution, Electrochim. Acta 48 (2003) 2767–2774.
[63] L.Q. Guo, S.X. Qin, B.J. Yang, D. Liang, L.J. Qiao, Effect of hydrogen on semiconductive properties of passive film on ferrite and austenite phases in a duplex stainless steel, Sci. Rep. 7 (2017) 3317.
[64] A. Kocijan, I. Milosev, B. Pihlar, Cobalt-Based Alloys for Orthopedic Applications Studied by Electrochemical and XPS analysis, (2004).
[65] A.W.E. Hodgson, S. Kurz, S. Virtanen, V. Fervel, C.O.A. Olsson, S. Mischler, Passive and transpassive behaviour of CoCrMo in simulated biological solutions, Electrochim. Acta 49 (2004) 2167–2178.
[66] J.F. Moulder, J. Chastain, Handbook of X-Ray Photoelectron Spectroscopy: A Reference Book of Standard Spectra for Identification and Interpretation of XPS Data: Physical Electronics Division, Perkin-Elmer Corporation, 1992.
[67] M. Honna, K. Mabuchi, K. Yoshida, S. Sakai, M. Ujihira, Effect of friction stroke length on damage and restoration of the passive film of cobalt chromium alloy, Kitasato Med. J. 47 (2017) 10–16.
[68] C. Donnet, J.M. Martin, T. Le Mogne, M. Belin, Super-low friction of MoS2 coatings in various environments, Tribol. Int. 29 (1996) 123–128.
[69] J.P.G. Farr, Molybdenum disulphide in lubrication. A review, Wear 35 (1975) 1–22.
[70] M. Lyvers, D. Bijukumar, A. Moore, P. Saborio, D. Royhman, M. Wimmer, et al., Electrochemically induced tribolayer with molybdenum for hip implants: Tribocorrosion and biocompatibility study, Thin Solid Films 644 (2017) 82–91.
[71] A.J.S. Peaker, J. Czernuszka, The Effect of Electric Field on the Formation of Hydroxyapatite Coatings, (1996).
[72] A. Neville, T. Hodgkiess, A.P. Morizot, Surface scales in sea water systems: effects of their formation on corrosion behaviour of engineering steels, Br. Corros. J. 32 (1997) 277–282.
[73] X. Zhang, M. Cresswell, Chapter 6 - calcium phosphate materials for controlled release systems, in: X. Zhang, M. Cresswell (Eds.), Inorganic Controlled Release Technology. Boston: Butterworth-Heinemann, 2016, pp. 161–187.